Inelastic proton scattering at 30–40 MeV from ^{12}C

R. De Leo, G. D'Erasmo, and A. Pantaleo
Dipartimento di Fisica dell'Universita di Bari, Bari, Italy
and Istituto Nazionale di Fisica Nucleare, Sezione di Bari, Bari, Italy

M. N. Harakeh
Kernfysisch Versneller Instituut, Groningen, The Netherlands
and Nuclear Physics Laboratory, University of Washington, Seattle, Washington 98195

E. Cereda, S. Micheletti, and M. Pignanelli
Dipartimento di Fisica dell'Universita di Milano, Milano, Italy
and Istituto Nazionale di Fisica Nucleare, Sezione di Milano, Milano, Italy
(Received 13 June 1983)

Elastic and inelastic proton differential cross sections for excitation of the following levels of ^{12}C: 2_1^+(4.43 MeV), 4_1^+(14.08 MeV), 0_2^+(7.65 MeV), and 3_1^-(9.64 MeV) have been measured at three incident energies between 30 and 40 MeV. The data have been described by coupled channel calculations and form factors obtained by coupling surface vibrations to static deformations. The reproduction of the 0_2^+ state data, if this state is assumed to be a β-vibrational state, requires a quadrupole β-vibrational amplitude which is 57% of the static quadrupole deformation and a mixing of the breathing mode of the nucleus with an amplitude that would correspond to about 1% of the $E0$ energy weighted sum rule. For the 3_1^- state it is found that the performed calculations are sensitive to the K projection, with the angular distribution of the 3_1^- state being better fitted assuming $K^\pi=3^-$ band. Coupled channel calculations using microscopic form factors obtained from wave functions generated using the resonating group method have also been performed and are compared to the experimental data.

[NUCLEAR REACTIONS $^{12}C(p,p')$, $E_p=29.95$, 35.2, and 39.9 MeV; measured $\sigma(E_x,\theta)$; compared with coupled channel analyses using rotor-vibrator model and microscopic 3-α cluster wave functions; deduced coupling parameters.]

I. INTRODUCTION

Recently an improvement has been achieved in the reproduction of differential cross sections obtained by inelastic scattering of hadrons from levels that are members of rotational bands built on γ,[1,2] β,[3] and octupole[4,5] vibrations in permanently deformed nuclei. In the γ vibration the nucleus retains the spheroidal equilibrium deformation of the ground state (g.s.), but in addition exhibits quadrupole oscillations such that ellipsoidal shapes are produced in the x-y plane ($K^\pi=2^+$ band). In the β vibration the nucleus exhibits quadrupole oscillations about a given equilibrium deformation, but retains its axial symmetry ($K^\pi=0^+$ band). In the octupole vibration the equilibrium deformation retains its axial symmetry ($K^\pi=0^-$, $J^\pi=1^-,3^-,5^-,\ldots$) or loses it in $K^\pi\neq0^-$ bands.

The improvement has been achieved in the framework of coupled channel (CC) calculations in which levels within the same band, g.s., β, γ, or octupole bands, are coupled together and treated in the framework of the usual rotational model allowing for different deformations for the different bands, but in addition each state of the g.s. band is also coupled to states of the β, γ, or octupole bands, with form factors derived from coupling the vibration in question to the static deformation. This model, hereafter referred to as "rotor vibrator," has been sufficiently tested as far as the γ vibration is concerned with different incident particles [α and ^{3}He (Ref. 1) and p (Refs. 2 and 6)] and for different incident energies [p from 20 (Ref. 6) to 800 MeV (Ref. 2)]

For the β and octupole vibrations in deformed nuclei little work has been performed and tests of the rotor-vibrator model are desirable. In heavy nuclei, e.g., apart from experimental difficulties in resolving the β-band levels due to the generally high density of levels even at the lower excitation energies, the rotor-vibrator model for the β band works[7] reasonably well. In principle, one can obtain a good description for the 0_β^+ band head of the β band once the β-vibrational amplitude $|\beta-\beta_2|$ is obtained from fitting the 2^+ member of the band. This can be complicated[3,8,9] by the mixing of the giant monopole resonance (GMR) into the low-lying 0^+ states, but this complication can be alleviated if the mixing matrix element and the location of the GMR are known. In light deformed nuclei ($A\lesssim40$) the tests of this model are made difficult by the fact that only a small percentage of the $E0$ monopole strength has been located[10] and moreover very little is known about the coupling matrix element be-

tween the GMR and the low-lying β vibration. Nevertheless, one can attempt to fit the states of the β band by searching for the admixture of the compressional mode [i.e., GMR] form factor to the vibrational mode form factor in the 0_1^+-0_2^+ excitation.

The ^{12}C is known to present a permanently deformed g.s., with a well developed g.s.-rotational band with states 0_1^+ (g.s.), 2_1^+ (4.43 MeV), and 4_1^+ (14.08 MeV). Moreover, the excited levels 0_2^+ (7.65 MeV), 3_1^- (9.64 MeV), and 1_1^- (10.84 MeV) could be interpreted[11] as the band heads of rotational bands, although it is not clear that these bands can all be considered as vibrational bands built on the deformed g.s.

The aim of this paper is to ascertain how valid this picture is from a comparison of inelastically scattered protons from ^{12}C at three incident energies between 30 and 40 MeV, a range high enough to ensure that compound nuclear contributions are negligible in the measured data. Details of the experiments are given in Sec. II. Unfortunately the 2_2^+ at 10.3 MeV and the 1_1^- at 10.84 MeV levels were not resolved (especially at forward angles for the 1_1^- state) from the background due to their large widths, and therefore no reliable experimental data are available for these states. In Sec. III a brief summary of form factors entering in the rotor-vibrator model is given and the evaluated cross sections are compared with the data to deduce the ^{12}C deformations.

Recently, Kamimura[11] evaluated the wave functions for many states studied here in the 3-α resonating group model (RGM). From these wave functions he evaluated all the transition densities between the levels of interest and these were found to reproduce nicely electron scattering data. By folding effective nucleon-nucleon interactions into these transition densities, it is possible to obtain nucleon induced transition potentials which if compared to our data can give information on the choice of the interaction or on the role played by CC effects in the excitations of low-lying states of ^{12}C. The result of this analysis is reported in Sec. IV and the conclusion of the paper is summarized in Sec. V.

II. EXPERIMENTAL METHOD

A proton beam from the AVF Milan cyclotron was momentum analyzed by a bending magnet and focused to a spot of 3—4 mm in diameter at the center of a 60 cm diam scattering chamber. Graphite foils of about 1 mg/cm^2 were used as targets. Their precise target thicknesses were determined by weighing and by measuring the energy loss in the foils of α particles from a ^{241}Am source. Three counter telescopes each made of two (2000 and 5000 μm) surface silicon detectors were used to measure angular distributions from 20° to 170° in steps of 5°. In Fig. 1, a typical spectrum taken at $E_p=29.95$ MeV and $\theta_{lab}=150°$ is shown. The overall energy resolution of the present experiment varied from 70 to 150 keV. Differential cross sections for the 0_1^+, 2_1^+, 0_2^+, 3_1^-, and 4_1^+ states were measured in this experiment at the following energies: $E_p=29.95$, 35.2, and 39.9 MeV. We have estimated the uncertainty in the target thickness to be of the order of 5—7 % and the total uncertainty in the cross section data

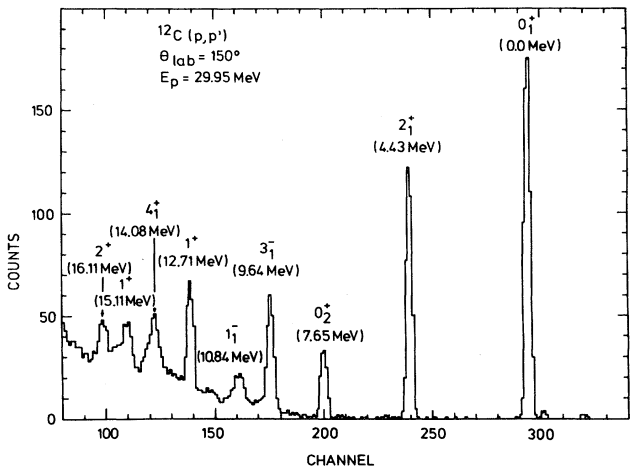

FIG. 1. A ^{12}C(p,p') spectrum taken at $E_p=29.95$ MeV and $\theta_{lab}=150°$. ^{12}C levels are labeled by J^π and excitation energy.

to be less than 10%. This estimate is larger for the 4_1^+ state (20% or even larger at angles where vertical bars appear on data points in Figs. 2—4) due to its larger width and the background subtraction procedure.

III. FORM FACTORS AND COUPLED CHANNEL ANALYSIS

A. Ground state rotational band

The experimental differential cross sections of the 0_1^+, 2_1^+, and 4_1^+ levels of the g.s. rotational band are shown (dots in Figs. 2—4) together with their fits (full curves in Figs. 2—4) obtained by using the code CHUCK (Ref. 12) to perform the CC calculations in the rotor-vibrator model and coupling the following levels 0_1^+, 2_1^+, 4_1^+, 0_2^+, 2_2^+, and 3_1^- (full coupling scheme shown schematically in the inset of Fig. 2) with form factors described in the next sections. Coulomb excitation and reorientation terms were taken into account in all the CC calculations described in this paper. Spin-orbit couplings were neglected, however, since it was found from a few test calculations that their effect on the cross section values was negligible and since very few analyzing power data are available.[13] The optical model (OM) potential parameters used in all these calculations are reported in Table I; these have been taken from Ref. 14, where they were obtained by a search using the rotational model, coupling only the 0_1^+ and 2_1^+ levels and averaging the values obtained at different incident energies between 20 and 40 MeV. The potential depths are energy dependent, a prescription that is customary when, as in this case, the excitation energy of the levels under investigation is a considerable fraction of the incident energy. The geometries of this OM potential are instead fixed with energy. For the form factors coupling two different states the average value of the optical potential depths in the two channels was used.

The deformation parameters used to obtain the full curves in Figs. 2—4, 6, and 8 are averages of values from

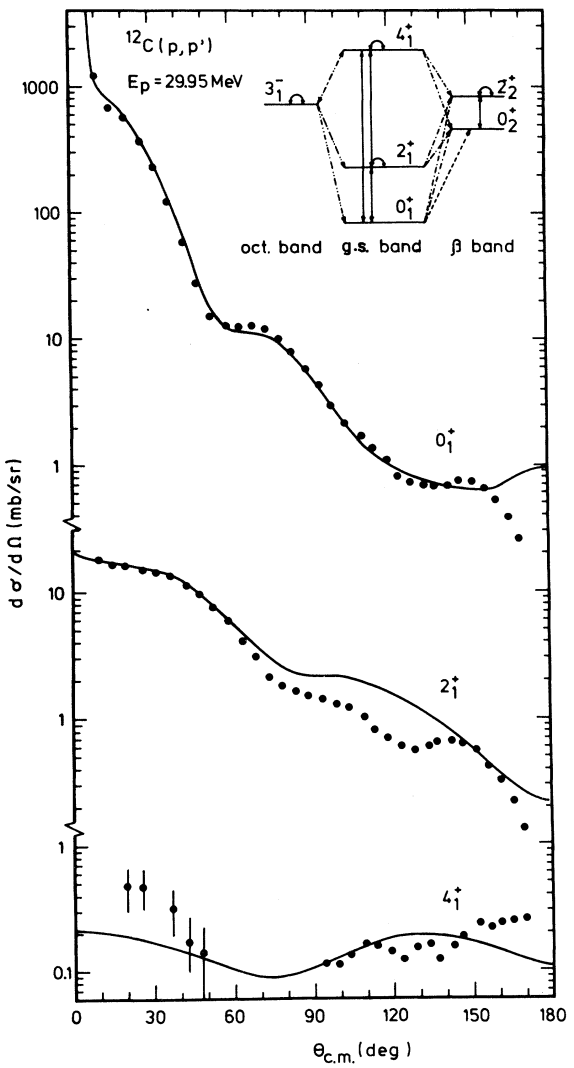

FIG. 2. Differential cross sections of the ^{12}C g.s. band 0_1^+, 2_1^+, and 4_1^+ states (dots) at $E_p = 29.95$ MeV. The full curves are the results of CC analyses in the rotor-vibrator model and with the full coupling scheme shown schematically in the inset. The form factors in the inset have the following meaning: ↔, rotational; ←·→, β vibration; ←··→, octupole vibration; and ←---→, monopole breathing mode. Optical model parameters from Table I and deformation parameters from Table II have been used. Vertical bars on data points represent statistical uncertainties only.

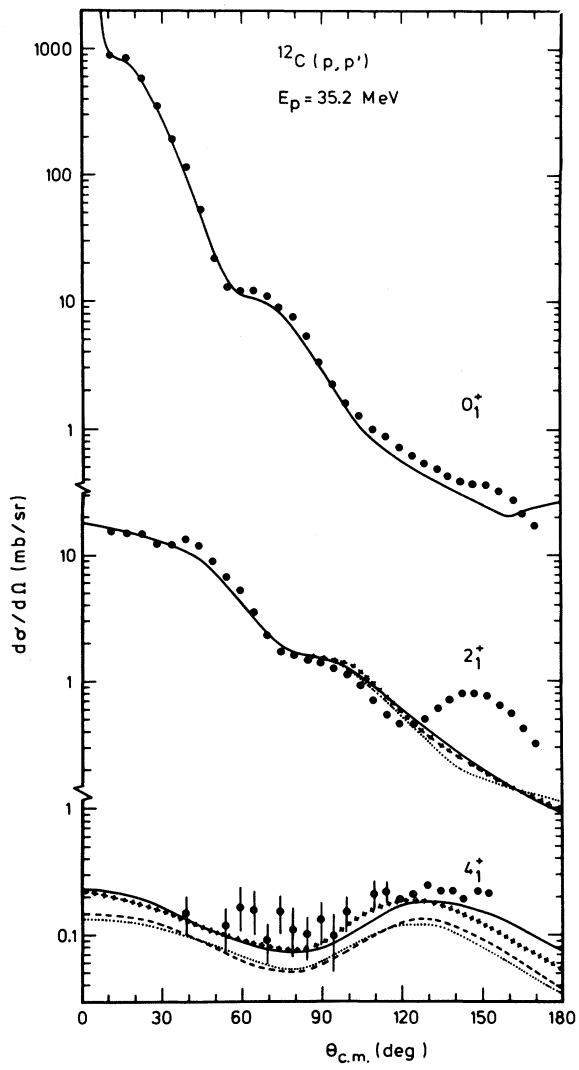

FIG. 3. Data same as in Fig. 2 for $E_p = 35.2$ MeV. Full curves refer to the full coupling scheme, crossed curves refer to the exclusion of the β band, dashed curves to the exclusion of the octupole band, and dotted curves to the exclusion of both bands.

fit search procedures performed at three incident energies on all the available cross sections. A preliminary search on the g.s. deformation parameters was performed with the program ECIS (Ref. 15) at the three different incident energies resulting in χ^2-weighted averages $\beta_2 = -0.663$ and $\beta_4 \cong 0.00$ (see also Table II). Some parameter values for the β band obtained at each energy are reported in Table II, while the χ^2-weighted averages over the bombarding energy for all these parameters are reported in the last row of Table II.

In Table III the average β_2 and β_4 values from our data analysis are listed together with other values obtained from analysis of hadron scattering[16–22] data taken with different projectiles at different incident energies. We have chosen to report in this table only deformation parameters from the literature obtained from CC analysis because of the strong CC effects expected in hadron inelastic scattering reactions on deformed nuclei. This table shows that a large variation in the quadrupole and hexadecapole deformations and deformation lengths is obtained in the different reactions. In this table the transition multipole moments for the states of the g.s. band obtained from hadron[16–22] and electron[23] inelastic scattering reactions and from theoretical calculations[11,24] are also listed. These will be discussed in more detail below.

The fits in Figs. 2–4 show that the large peak at back-

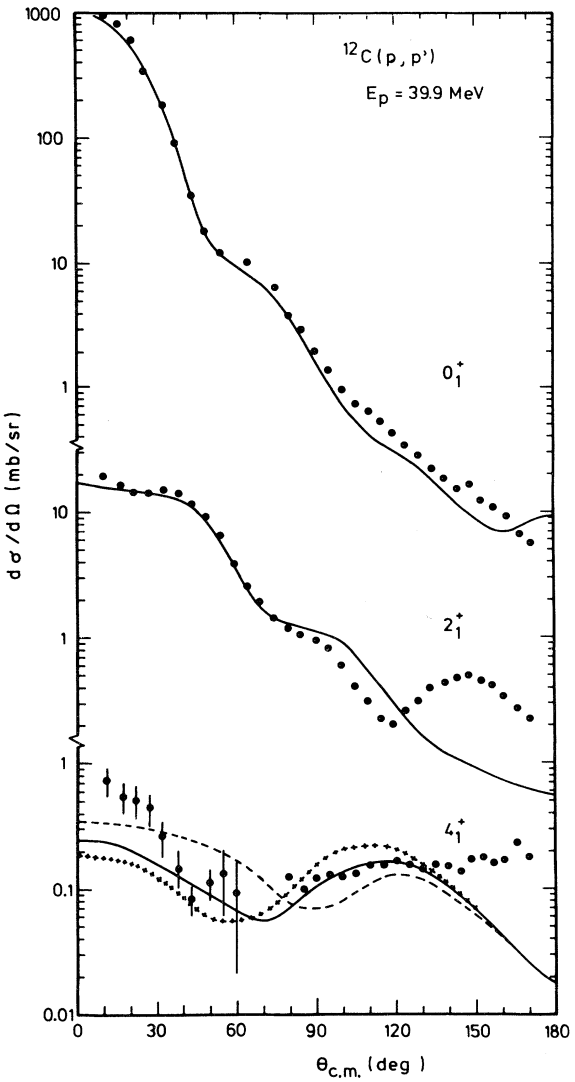

FIG. 4. Same as Fig. 2 for $E_p=39.9$ MeV. Full curves refer to deformations in Table II ($\beta_4=0.0$); the dashed curve shows the variation in the predicted 4_1^+ state assuming $\beta_4=-0.05$, and the crossed curve for $\beta_4=+0.05$.

ward angles in the 2_1^+ cross sections at 35 and 40 MeV, but weak at 30 MeV, is not reproduced by the calculations. This peak is, however, noticeably weaker in the elastic cross sections and thus it is probably not due to the coupling, here neglected, with high excited levels,[25] namely giant resonance states. This conclusion is derived from

TABLE I. Optical model parameters in the usual notation (depths in MeV and lengths in fm) used in all CC calculations described in this paper.

$V_0=(59.0-0.34.E_p)$	$r_0=1.064$	$a_0=0.623$
$W_v=0$	$r_w=1.2$	$a_w=0.6$
$W_s=(0.5+0.125.E_p)$	for $E_p<28$ MeV	
$W_s=4.0$	for $E_p>28$ MeV	
$V_{so}=6.0$	$r_{so}=1.0$	$a_{so}=0.6$
	$r_C=1.2$	

TABLE II. Deformation parameters related to the 0_2^+ band deduced at the three incident energies and their χ^2-weighted averages. The χ^2-weighted averages over the three incident energies for β_2 and β_4 used in the CC calculation to obtain the β-band deformation parameters are -0.663 and 0.00, respectively; the χ^2-weighted average for η_{33} is 0.35 (see the text for more details).

E_p (MeV)	$\lvert\beta-\beta_2\rvert$	β_2^β	β_0
29.95	0.29	3.3	0.048
35.2	0.38	3.7	0.058
39.9	0.47	3.9	0.054
χ^2-weighted averages	0.38	3.7	0.054

Ref. 25 in which it was found that such coupling affects in the same way the 0_1^+ and the 2_1^+ states.

The effect on the states of the g.s. band due to neglection of the couplings of the octupole band (dashed curves), or the couplings of the β band (crossed curves), or of the couplings of both bands (dotted curves), is shown in Fig. 3. Only the 4_1^+ state results are affected by the exclusion of only the octupole band; its cross section remains underestimated over the whole angular range, and the fit cannot be restored by a variation of β_4, the hexadecapole deformation of the g.s. band that the fit search procedures have ascertained to be very small (Table II). In fact either an increase or a decrease in β_4 shifts the minimum of the calculated 4_1^+ cross section out of phase with the minimum of the experimental data (see Fig. 4), and increases the calculated curves only in one half of the angular range while decreasing them in the other half in disagreement with the data.

We note that β_2 in Table II is higher than the values deduced in previous searches[14,25,26] performed without the inclusion of the 4_1^+ cross section data in the fit procedures. Moreover as a consequence of the searches we have made we deduce that important processes feeding the ^{12}C 4_1^+ state are two-step excitations through the 2_1^+ and 3_1^- levels. This, in fact, brings into question analyses of inelastic hadron scattering data that report large β_4 values without having taken the effect of the 3_1^- state coupling into consideration.

B. β-vibration rotational band

In these calculations the 0_2^+ and 2_2^+ states are assumed to be members of the same rotational band, and moreover it is assumed that this band is the one built on a β vibration of the g.s. There are several theoretical works that justify the first assumption, as for example, the 3-α RGM calculation[11] in which it was found that the mass densities of the 0_2^+ and 2_2^+ states are very similar. However, this model[11] predicts a large change in the nuclear shape in going from the g.s.-band levels, with a rms of 2.40 fm and with a peak in the monopole mass density distribution at 1.2 fm, to the 0_2^+ and 2_2^+ levels that instead show a smoothly decreasing density distribution with a larger rms of 3.47 fm (see Fig. 2 of Ref. 11). The 3-α cluster model classifies the g.s.-band levels as shell-model—like states,

TABLE III. Quadrupole and hexadecapole deformation parameters, deformation lengths ($\delta=\beta R$)[a] and transition multipole moments for ^{12}C.

Experiment or theory	β_2; δ_2 (fm)	β_4; δ_4 (fm)	$ME(E2)$ e fm^2	$ME(E4)$ e fm^4	Ref.
n, 14.1 MeV[b]	−0.6; −1.72		−6.7		16
p, 5–8 MeV[c]	−0.5; −1.43		−7.3		17
p, 800 MeV[d]	−0.652; −1.36	0.048; 0.1			18
p, 800 MeV[e]	−0.90; −1.91	0.001; 0.002	−6.0	21.9	19
p, 800 MeV[f]	−0.78; −1.70	0.001; 0.002	−6.17	23.2	20
p, 30–40 MeV	−0.663; −1.62	0.00; 0.00	−7.26	32.0	present work
d, 60–90 MeV[g]	−0.477; −1.36	0.0; 0.0	−6.97	28.5	21
α, 65 MeV[h]	−0.4; −1.47	0.16; 0.59	−9.4	123.7	22
e, 183–250 MeV[i]			−6.34	21.5	23
H-F[j]			−6.88	29.4	24
3-α RGM[k]			−6.81	30.3	11

[a] The deformation length is $\delta=\beta R$, where $R=r_0A^{1/3}$ fm except for the 800 MeV proton data $R=r_wA^{1/3}$ fm. r_0 and r_w are the real and imaginary reduced radii of the optical potential.
[b] The 4^+ state was not considered in the analysis. The real geometrical parameters of the optical potential are $r_0=1.25$ and $a_0=0.35$.
[c] The 4^+ state cannot be excited at these bombarding energies. The real geometrical parameters used are $r_0=1.25$ and $a_0=0.65$.
[d] Initial analysis of the 800 MeV data; no multipole moments are given since the fits were not optimal.
[e] The values quoted here for the multipole moments have been recalculated and are different, apparently due to an error, from the values given by Ref. 19; the geometrical parameters used are $r_w=0.925$ and $a_w=0.40$.
[f] Recent analysis of the 800 MeV data with the program ECIS; the geometrical parameters used are $r_w=0.951$ and $a_w=0.489$.
[g] Average values over the incident energies of Ref. 21; the geometrical parameters used are $r_0=1.25$ and $a_0=0.64$.
[h] The geometrical parameters used are $r_0=1.6$ and $a_0=0.61$.
[i] The transition densities were obtained from a Nilssøn model analysis.
[j] H-F refers to Hartree-Fock calculations.
[k] 3-α RGM refers to 3-α resonating group method calculations.

and the 0_2^+ and 2_2^+ levels as molecular states due to the large differences found in the spatial distribution of the three alphas in the two bands (see the discussion in Ref. 11). This in fact argues against assuming the 0_2^+ to be a β vibrational or a breathing mode state.

In the following a brief description of the form factors entering the rotor-vibrator model, as applied to the β band, is given. The coupling of a β-quadrupole vibration with amplitude $|\beta-\beta_2|$ to a static deformation (β_2, β_4, and higher order deformations) results in a parametrization of the nuclear radius as

$$R(\Omega')=R_0\left[1+\sum_\lambda \beta_\lambda Y_\lambda^0(\Omega')+|\beta-\beta_2|\,Y_2^0(\Omega')\right]. \quad (1)$$

Following Refs. 1 and 3, we expand the potential in terms of $|\beta-\beta_2|$ up to first order and then expand the zeroth and first order terms in terms of multipoles. After rotating to the fixed frame, one can obtain the form factors for excitation within the same rotational band,

$$f_{\lambda 0\lambda}(r)=\beta_\lambda v_\lambda^{(0)}(r)\langle IK\lambda 0\,|\,I'K'\rangle(-1)^{I-I'}\delta_{KK'}\,, \quad (2)$$

and the ones that connect the states of the g.s. band to the states of the β band (Refs. 1 and 3),

$$f_{\lambda 0\lambda}(r)=(-1)^\lambda\langle I_\beta 0\lambda 0\,|\,I_g 0\rangle\frac{1}{\sqrt{4\pi\hat{\lambda}}}\sum_l \hat{l}v_l^{(1)}(r)(\sqrt{5}\,|\beta-\beta_2|\,\langle l020\,|\,\lambda 0\rangle^2-\xi\langle l000\,|\,\lambda 0\rangle^2)\,. \quad (3)$$

For the definition of the symbols see Refs. 1 and 3. The second term in the parentheses of Eq. (3) is added to satisfy the condition of conserving the number of particles,

$$\int f_{000}(r)r^2dr=0\,. \quad (4)$$

The breathing mode form factor for the 0_1^+-0_2^+ excitation was taken of the form[27]

$$f_{000}(r)=\beta_0\left[-3U(r)-r\frac{dU(r)}{dr}\right], \quad (5)$$

where U is the OM potential.

In Fig. 5, the real part of the breathing mode form factor is compared to the real part of the β-vibration form factor. It is clear from this figure that the breathing mode form factor (dashed curve) which is essentially a volume oscillation is peaked more inward than the β-vibration monopole form factor (dotted curve) which has a node at a larger radial distance than that of the breathing mode form factor and peaks further out in the nuclear surface. The form factor which is used in the final analysis of the 0_2^+ data (solid curve) as will be discussed shortly is a combination of these two form factors. It has a node and peaks at a larger radial distance than the breathing mode form factor in agreement with the characteristics of the monopole transition density obtained for this 0_2^+ state by Kamimura[11] in the 3-α RGM microscopic calculation.

The free parameters coming from the inclusion of the β band in the CC calculations are the following: $|\beta-\beta_2|$ [from Eq. (3); in this equation ξ is not a free parameter but is a function of $|\beta-\beta_2|$], β_2^β [from Eq. (2)] that is the quadrupole deformation of the β band, and the breathing mode deformation parameter β_0 [from Eq. (5)]. A search on these three parameters, obtained with a 0_1^+, 2_1^+, 0_2^+, 2_2^+, coupling scheme and minimizing the χ^2 fit to their data, resulted in the values listed in Table II and the fits in Fig. 6 shown as dashed curves; their averages over the three incident energies are also reported in Table II and the fits in Figs. 2–4 and 6 with full curves (obtained in the full coupling scheme).

We note that the general shape and absolute values of the 0_2^+ cross sections in Fig. 6 are reproduced by the dashed curves, in particular. Some tests were performed to ascertain if some couplings could be omitted from the full coupling scheme. These produced as expected a worsening of the fit in the same way as found in Ref. 3. Some of the tests for the 35 MeV case are reported in Fig. 7. The full curve represents the calculated curve for the 0_2^+ obtained with the full coupling scheme (best fit parameters from Table II). The crossed curve refers to the exclusion of the 4_1^+ and 3_1^- levels from the full coupling scheme. This exclusion influences slightly only the backward part of the 0_2^+ cross section. The exclusion of the 2_2^+ level (long-dashed curve) influences the whole angular range, and moreover indicates that this coupling is the only one useful in reproducing the increasing trend of the experimental data at backward angles. The dotted-dashed curve refers to the exclusion of the 2_1^+ level in addition, and hence refers to only the 0_1^+-0_2^+ coupling with the same form factor as obtained from the best fit in the full CC scheme (i.e., the combination of breathing mode and β-vibration form factors with deformations as listed in Table II). The short-dashed and dotted curves refer to distorted wave Born approximation (DWBA) calculated curves with only either the β vibration or the breathing mode form factors, respectively.

The $|\beta-\beta_2|$ value in Table II suggests that in ^{12}C the quadrupole β vibration is a large percentage (57%) of the static axial quadrupole deformation β_2; indeed this seems to be a strong vibration if compared to 18% obtained in Ref. 3 for ^{24}Mg or to the still lower value of 7% found in

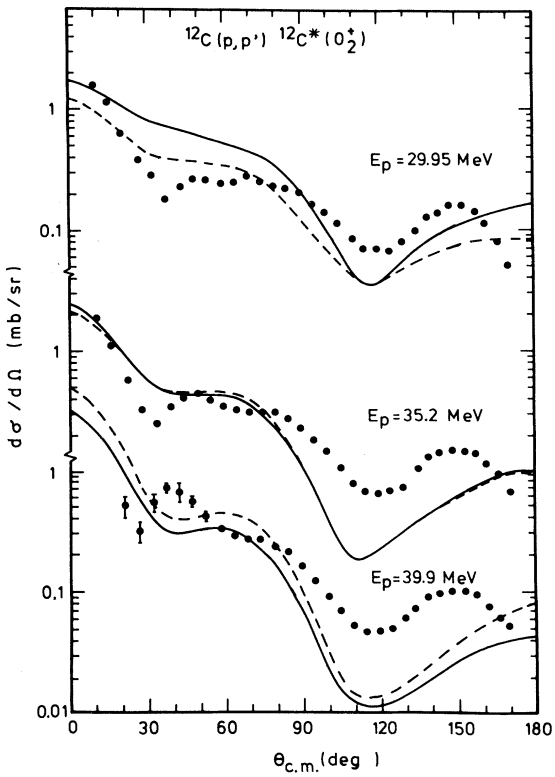

FIG. 6. Cross sections of the 0_2^+ level of ^{12}C at the quoted energies; the full curves have the same meaning as those of Fig. 2 and refer to the χ^2-weighted average parameters from Table II; the dashed curves refer to the best fit parameters at the corresponding bombarding energies from Table II.

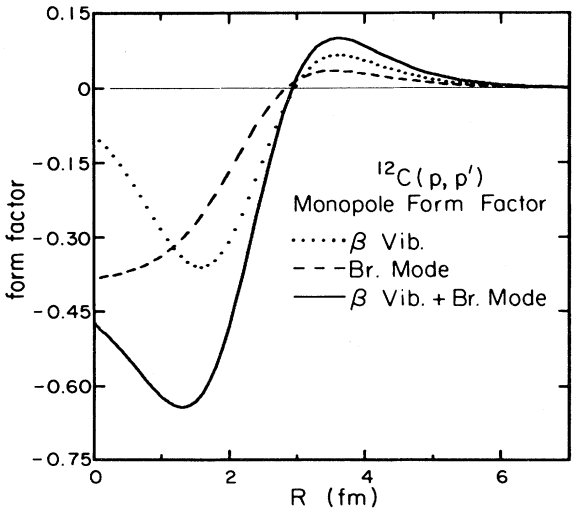

FIG. 5. Monopole form factors for excitation of the 0_2^+ state. All form factors are multiplied by $(2\mu/\hbar^2)$ where μ is the reduced mass for the reaction. The dotted curve refers to the β-vibration form factor [Eq. (3)], the dashed curve to the breathing mode form factor [Eq. (5)], and the solid curve to the combination of β-vibration and breathing mode form factors with the χ^2-weighted average coupling parameters of Table II.

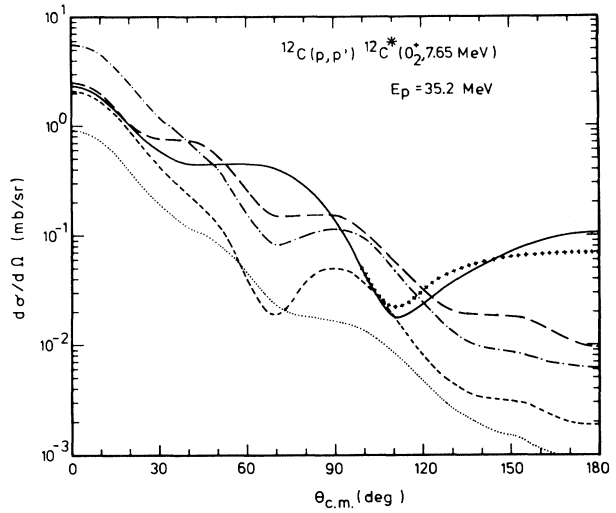

FIG. 7. Influence of the various couplings in the CC scheme on the calculated 0_2^+ cross section. The full curve has been evaluated with the best fit parameters from Table II and using the full coupling scheme; the crossed curve refers to the exclusion of the 4_1^+ and 3_1^- states; and the long-dashed and dotted-dashed curves to the exclusion of also the 2_2^+ and $2_2^+,2_1^+$ levels, respectively. The short-dashed and the dotted curves refer to DWBA calculations with only either the vibrational or the compressional 0_1^+-0_2^+ form factors, respectively.

Ref. 7 for ^{152}Sm.

The β_2^β quadrupole deformation of the β band in Table II is large (3.7) compared with the prediction[1] obtained from β_2 by scaling the moments of inertia of the g.s. and β bands (0.9). Indeed it is rather interesting that the fit to the 0_2^+ data requires a very large and positive β_2^β about five times that of the ground state. This turns out to be in agreement with the 3-α RGM calculation of Kamimura[11] who predicts that the deformation of the 0_2^+ band is 3—4 times that of the ground state which can be explained as due to the completely different structures of the 0_2^+ band and the g.s. band. This may in fact raise the question as to whether our analysis of the 0_2^+ state as the band head of a β band is reasonable. Yet, because of our parametrization and the way the χ^2 search for the free parameters $|\beta-\beta_2|$, β_0, and β_2^β is carried out, we are left with enough freedom to obtain a good transition density to the 0_2^+ state. It seems, moreover, that this χ^2 search procedure determines sensitively the β_2^β parameter. In the case of ^{24}Mg for example, the search which included the data of both the 0_β^+ and the 2_β^+ levels resulted[3] for the 0^+ band with a band head at 6.43 MeV in a β_2^β similar to the β_2 of the g.s., thus indicating the correct nature of the band to be a β-vibrational band built on the g.s. of ^{24}Mg. In the case of ^{12}C, however, no data were available for the 2_2^+ state which can make our results for the derived β_2^β value and therefore to the nature of the excited 0^+ band less conclusive. Nevertheless, a good test of the meaningfulness of our analysis can be obtained from a comparison of the derived multipole transition moments connecting the g.s. band to the 0_2^+ band to those obtained from electromagnetic measurements. For example, the $ME(E0)$ value connecting the 0_1^+ to the 0_2^+ obtained from this analysis is 4.0 e fm^2 in good agreement with that obtained from electron scattering,[28,29] 4.38 ± 0.2 e fm^2 [5.37 ± 0.22 e fm^2 is reported in Ref. 30]. Also the $BE(E2;0_2^+\rightarrow2_1^+)$ connecting the 0_2^+ to the 2_1^+ is from our analysis 11.6 e^2fm^4 compared to 13 ± 4 e^2fm^4 obtained from the literature[29] (see also Table IV).

C. Octupole vibration rotational band

The mass distribution of the 3_1^- state calculated in Ref. 11 came out considerably different from that of the 1_1^- state at 10.84 MeV. This result suggests that these two states belong to different octupole bands with $K^\pi=3^-$ and 0^-, respectively, of which these states are the band heads. Unfortunately, the data for the 1^- state were of low quality which makes it impossible to draw any conclusions from their analysis. For the 3^- state, however, we can test whether its differential cross section can be described with the rotor-vibrator model CC calculations.

The form factors for an octupole vibration built on a permanent deformation are derived in a way similar to that described for the β vibration in Sec. III B. The substitution of an octupole vibration instead of a quadrupole β vibration term in Eq. (1) leads to the following:

$$R(\Omega')=R_0\left\{1+\sum_\lambda\beta_\lambda Y_\lambda^0(\Omega')+[\alpha_{3K}Y_3^K(\Omega')+\alpha_{3-K}Y_3^{-K}(\Omega')]\right\}. \quad (6)$$

K can assume the values from 0 to 3. The form factors which lead from the states of the g.s. band to states of the octupole band are then[1,4]

TABLE IV. Transition multipole moments connecting the β-band and octupole band levels to the g.s.-band levels of ^{12}C.

$ME(E0)$	$ME(E2,0_2^+\rightarrow2_1^+)$	$ME(E3)$	Ref.
4.0	3.4	26.3	present work
		23.9	16[a]
		18.5	19[b]
		19.5	21[c]
4.38 ± 0.2		27.5	28
5.37 ± 0.22			30
	3.6 ± 0.6		29
6.7	2.4	29.5	11[d]

[a] $\eta_{33}=0.33$.
[b] The analysis of the 3^- cross section was performed in DWBA with $\beta_3=0.585$ and $r_w=0.903$ fm and $a_w=0.528$ fm.
[c] In calculating the $ME(E3)$ from the β_3 parameter of 0.2 given by Ref. 21 we assumed they used $K^\pi=3^-$, if instead $K^\pi=0^-$ was used by Ref. 21 the $ME(E3)$ value would be 12.1 e fm^3.
[d] Results of the 3-α RGM calculations.

$$f_{\lambda 0\lambda}(r)=(-1)^{\lambda}\langle I-K\lambda K \mid I_g 0\rangle \frac{1}{\sqrt{4\pi}\hat{\lambda}} \times \sum_l \hat{l} v_l^{(1)}(r)(\sqrt{7}\eta_{3K}\langle l030 \mid \lambda 0\rangle\langle l03\pm K \mid \lambda\pm K\rangle - \sqrt{3}\xi_K\langle l010 \mid \lambda 0\rangle\langle l01\pm K \mid \lambda\pm K\rangle) , \quad (7)$$

where

$$\eta_{3K}=\left[\frac{2}{1+\delta_{K0}}\right]^{1/2}\langle \chi_0(\zeta) \mid \alpha_{3K} \mid \chi_K(\zeta)\rangle \quad (8)$$

and where $\chi(\zeta)$ are the intrinsic wave functions of the rotational bands. The term in ξ is the correction for the spurious motion of the center of mass introduced by only the $K^{\pi}=0^-$ and 1^- octupole vibrations. ξ is not a free parameter since it is completely determined once η_{3K} is, by the condition of translational invariance,

$$\int f_{101}(r) r^3 dr = 0 . \quad (9)$$

In these calculations the quadrupole deformation of the octupole rotational band, β_2^{oct}, is not varied and is assumed to be equal to that of the g.s. band.

We have performed two complete coupling calculations giving to K the two possible values 0 and 3. The results are reported in Fig. 8. We note that the $K^{\pi}=0^-$ dotted-dashed curve does not reproduce the 30 MeV data around 100°. On the other hand, the calculated differential cross section assuming $K^{\pi}=3^-$ for the 3^- state (full curves in Fig. 8) reproduce the data in the whole angular interval. This result is in agreement with Refs. 11 and 31 suggesting $K^{\pi}=3^-$ for the 3_1^- level. The average η_{33} value with which the full curves in Fig. 8 have been evaluated, is reported in Table II. This corresponds to a $ME(E3)$ value of 26.3 $e\,\text{fm}^3$ in very good agreement both with electromagnetic measurements[28] and with theory[11] (see also Table IV). If on the other hand $K^{\pi}=0^-$ was assumed, we deduce for η_{30} a 30% higher value from the dotted-dashed fits.

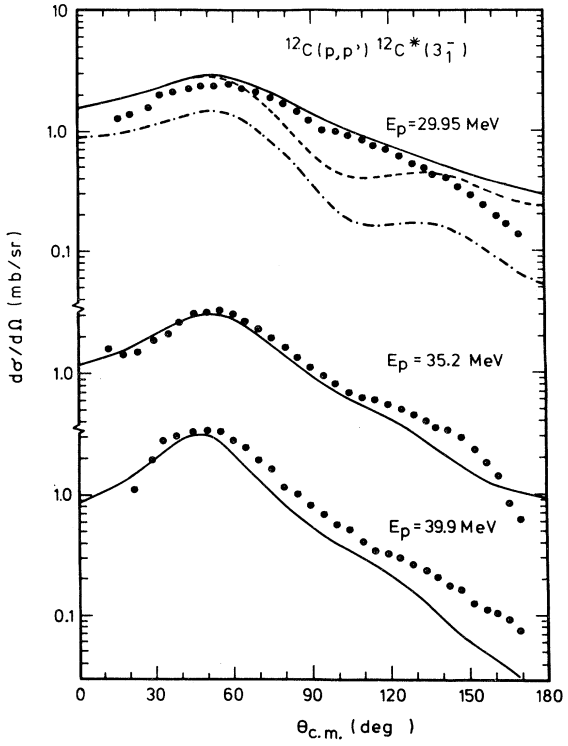

FIG. 8. Cross sections of the 3_1^- level of ^{12}C (dots) at the quoted energies with the calculations obtained using the rotor-vibrator model, the full coupling scheme, and assuming $K^{\pi}=3^-$ (full curves), or 0^- (dotted-dashed curve). The dashed curve represents the modification to the full curve when the 2_1^+ level is excluded from the coupling scheme.

To finish this section it is useful to check which couplings are important for the exact reproduction of the 3_1^- data among those considered in the full coupling scheme. Assuming $K^{\pi}=3^-$ it turns out that the 2_1^+-3_1^- coupling is very important in reproducing the 3_1^- differential cross section. Its exclusion gives the dashed curve in Fig. 8 which is similar to the dotted-dashed curve evaluated for $K^{\pi}=0^-$ and does not reproduce the experimental data around 100°; the η_{33} value extracted from this last analysis is very near to the one in Table II indicating that the 2_1^+ coupling is important to reproduce the exact shape of the 3_1^- cross section, but not its magnitude. Similarly neglecting the reorientation term for the 3_1^- level leads to a worsening of the fit (not shown here).

We note that in the experimental data of the 0_1^+ g.s. and the 3_1^- level no conspicuous backward peaks, similar to the unreproduced backward peaks in the 2_1^+ and 0_2^+ cross sections at 35 and 40 MeV, are present.

IV. α-CLUSTER CALCULATIONS

In this section we compare our experimental data with CC calculations in which the transition potentials are obtained by folding effective nucleon-nucleon interactions into mass transition densities of ^{12}C levels evaluated with the 3-α RGM wave functions.[11] The aim is to select among different effective interactions the best one to use for evaluating transition potentials from transition densities at these bombarding energies and to compare these CC calculations with collective model ones in Sec. III. The first aim finds its motivation in the work of Ref. 11, which showed that radial shapes of the transition potentials are strongly dependent upon the nucleon-nucleon interaction.

Following Ref. 11 we examine four interactions, namely a Blatt-Jackson[32] interaction (hereafter labeled as I), a Volkov[33] interaction (II), a Hasegawa-Nagata[34] interaction (III), and a $M3Y$ interaction (IV) used by Satchler and Love[35] which includes a δ-interaction term to take care of exchange effects. Our tests are confined to only the v_{00} components of these interactions, since the contributions from the v_{10}, v_{01}, and v_{11} terms vanish[11] in the folding

due to the saturation of spin and isospin in the used wave functions. We consider, moreover, a simple Yukawa interaction obtained[36] without considering the repulsive part coming from exchange contributions:

$$\text{(V)}: \quad v_{00}(s) = -35\exp(-s)/s \ .$$

Here s refers to the projectile-nucleon distance. The strength and range of this interaction were obtained[36] by reproducing the absolute value of the 2_1^+ cross section in ^{12}C taken with protons at 65 MeV. We consider also a renormalized version of the (IV) interaction with the same volume integral of the (V) interaction:

$$\text{(VI)}: \quad v_{00}(s) = 7999\exp(-4s)/4s - 2134\exp(-2.5s)/2.5s + \text{exchange term} \ .$$

The possibility of renormalizing the depth of the interaction to offset the neglection of other channels or the lack in the calculations of antisymmetrization between projectile and target nucleons was outlined in Ref. 11. However, in the calculations to be described below all couplings were taken into account. Therefore any need for renormalization of the interaction strengths would arise from the neglection of exchange effects which applies for interactions (I), (II), and (III) only. In a first trial, we evaluated all OM and transition potentials by folding the various projectile-nucleon interactions into the mass and mass transition densities. The full CC calculations resulted in bad fits to all the available data (not shown here). We therefore finally decided to take the phenomenological OM potentials and obtain by folding only the transition potentials. Since we did not have a good prescription to obtain the imaginary part of the transition potential from folding, we took this part from the phenomenological OM potential as described in Sec. III for the various bands. With these transition potentials full CC calculations were then performed for the 2_1^+, 0_2^+, and 3_1^- levels at 30 MeV. The results are displayed in Figs. 9 and 10.

Using interaction (IV), we have first tested the effect of neglecting the imaginary collective part of the transition potentials. In Fig. 10 curves IV refer to its inclusion, curves VII to its exclusion. An overall worsening of the fit to the 2_1^+ level data due to the exclusion of the imaginary part of the transition potential is observed: The 3_1^- cross sections are not greatly affected from its exclusion, but for the 0_2^+ level, although a relative improvement is obtained for the backward angles, a worsening of the fit is observed at the forward angles. Because of the significant differences observed, all other CC calculations were performed, including imaginary transition potentials.

Inspecting Figs. 9 and 10, one observes that, in general, the data are fairly reproduced using transition potentials obtained by folding the Blatt-Jackson (I) interaction or the $M3Y$ interaction with its variations (IV) and (VI) or the simple Yukawa interaction (V). In particular, insignificant differences are observed for curves (IV) and (VI) referring to the respective potentials. The transition potentials obtained by folding a Volkov interaction (II) or a Hasegawa-Nagata interaction (III) do poorly in fitting the absolute magnitudes of the cross sections.

Disregarding the renormalizations, however, the comparison among the curves (I) to (IV) does not show substantial differences if one excludes the observation that the Volkov and Hasegawa-Nagata interactions produce minima in the diffraction patterns that come slightly earlier than the experimental data indicate. The interaction that instead produces overall slightly better fits than the others and that qualitatively and quantitatively better reproduces the data, at least for the 2_1^+ and 3_1^- states, is the simple Yukawa (V) interaction. Its fits are very similar to those obtained in the collective analysis of Sec. III. All the interactions fail in reproducing the 0_2^+ data at angles greater than 40° where the calculations are far below the experimental points. In this respect, the collective model description seems to be doing better in describing the 0_2^+ excitation as shown in Sec. III. There it was also found that the deduced

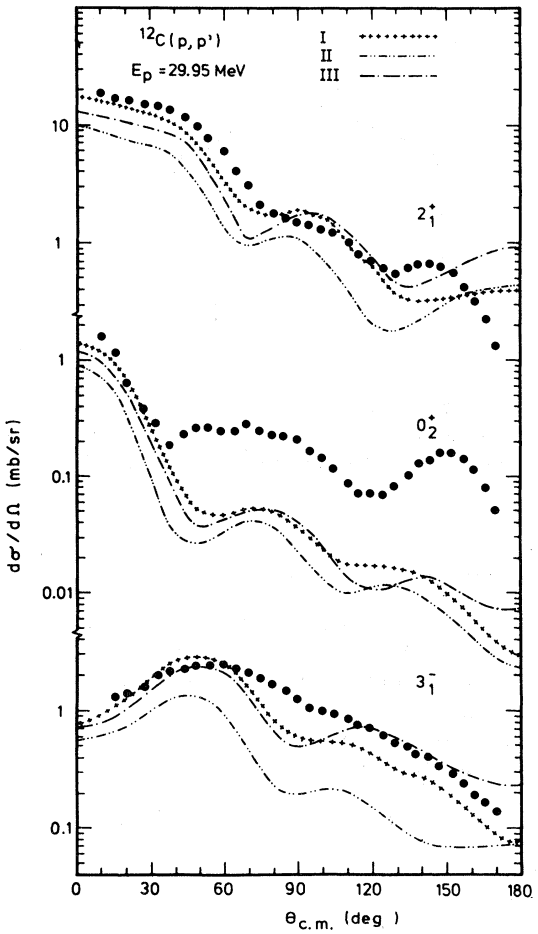

FIG. 9. The same calculations that produced the full curves in Figs. 2—4, 6, and 8 have been repeated using microscopic transition potentials obtained from folding various nucleon-nucleon interactions into the microscopic transition densities from Ref. 11. Three different nucleon-nucleon interactions, denoted with the same Roman numbers as in the text, have been used. See the text for more details.

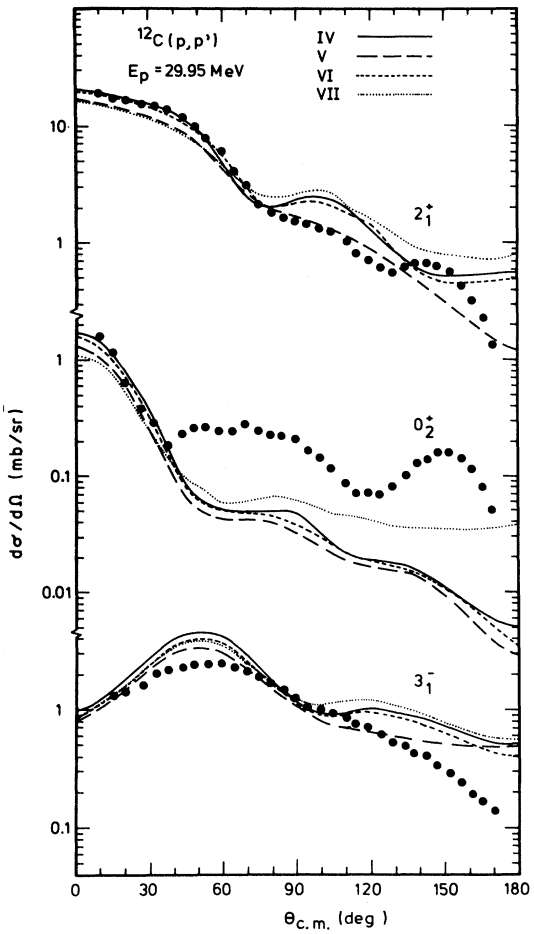

FIG. 10. Same as Fig. 9 for other nucleon-nucleon interactions, denoted IV to VI. The dotted curve VII refers to the same calculation as for IV but with the imaginary coupling dropped.

$$BE(E2;0_2^+ \rightarrow 2_1^+) = 11.6\ e^2\,\mathrm{fm}^4$$

is larger than that predicted (5.6 $e^2\,\mathrm{fm}^4$) by the 3-α RGM calculation.[11] Therefore the underestimation of the 0_2^+ cross section could be due to a deficiency in the microscopic transition density, which may be the reason why in Ref. 36 the 0_2^+ cross section was hardly affected when the 2_1^+ to 0_2^+ coupling was neglected.

V. DISCUSSION AND CONCLUSION

In the previous sections we presented the differential cross sections for the g.s., 2_1^+, 0_2^+, 3_1^-, and 4_1^+ levels in ^{12}C measured at incident proton energies of 29.95, 35.2, and 39.9 MeV. The data were compared with CC calculations obtained using the rotor-vibrator model and coupling the g.s., β, and octupole bands with the coupling scheme shown in the inset of Fig. 2. The g.s.-band data were found to be satisfactorily reproduced if the g.s. is assumed to have an oblate deformation with $\beta_2 = -0.663$ and $\beta_4 \cong 0.0$. If the coupling with the other bands is neglected, only the 4_1^+ level remains unreproduced since a strong contribution to this level is coming from the octupole band. The good fit cannot be regained by introducing a hexadecapole deformation since it was demonstrated in Sec. III A that even a small positive or negative hexadecapole deformation ($\beta = \pm 0.05$) leads to a deterioration of the fit of the 4_1^+ data. We can compare the results obtained from our analysis to those obtained from other experiments with various projectiles at various incident energies. This is done in Table III. Only results of hadron scattering data analyzed in a CC framework are reported in this table. It is quite apparent from inspection of Table III that there is a large variation in the deformation parameters. This variation is not removed by comparing deformation lengths instead. Following a suggestion by Mackintosh[37] based on a theorem by Satchler[38] relating multipole moments of folded form factors and potentials to those of transition and g.s. densities, we have calculated[1] the multipole moments of the real parts of the form factors of Eq. (2) for all the reported CC analyzed hadron scattering data in the literature. In the case of 800 MeV proton data, the imaginary geometry was used instead because it has the largest contribution to the excitation cross section. The quadrupole and hexadecapole moments so obtained (see Table III; here $ME(E\lambda) \equiv [BE(E\lambda)]^{1/2}$) are in very good agreement with each other and with those obtained from electron scattering data. The only exception to this good agreement being the multipole moments obtained from the CC analysis[22] of inelastic α-scattering data at $E_\alpha = 65$ MeV which predicts a large hexadecapole moment in contradiction with the results of all other hadron scattering data and also in contradiction with the Nilssøn model analysis of the electron scattering[23] data from ^{12}C. In this analysis[23] it was found that the quadrupole and hexadecapole deformation parameters are dependent on the nuclear radius with $\beta_4 \cong 0.01$ near the nuclear surface to which hadron scattering is most sensitive. We note also that the quadrupole and hexadecapole multipole moments predicted by Hartree-Fock[24] and 3-α RGM (Ref. 11) calculations are in good agreement with our results.

The energy dependence of the cross section of the 0_2^+ level at 7.65 MeV has been reproduced using a combination of β-vibration and breathing mode form factors. A large $|\beta - \beta_2|$ coupling parameter is required which amounts to 57% of the static quadrupole deformation of the g.s. Moreover, a weak contribution of the compressional $E0$ mode, with an amplitude that would correspond to 1% of the $E0$ energy weighted sum rule (EWSR), is necessary. The combined form factor is similar in shape to that predicted from the 3-α RGM calculations of Kamimura.[11] These results are in contrast with the analysis of Ref. 9 which explained the 0_2^+ cross section measured in ^{12}C(α,α') essentially by the compressional $E0$ mode only. We have also deduced the quadrupole deformation of the β band which turned out to be of opposite sign and four times larger than the value estimated by scaling the g.s. quadrupole deformation parameter through the ratio of the moments of inertia of the β and g.s. bands. However, a large uncertainty has to be associated with the β_2^β since the 2_2^+ cross section data to which the β_2^β is very sensitive were lacking in the fit procedure. A large value of the β_2^β was also predicted by the 3-α RGM calculation of Kam-

imura[11] who predicts the β band to be of completely different nature from the g.s. band, i.e., molecular versus shell-model–like, respectively. The multipole moments connecting the 0_2^+ state to the g.s.-band states were obtained from the real parts of the form factor (3) [for $ME(E0)$ a combination of form factors (3) and (5) as they appear in the analysis of our data was taken] and are listed in Table IV. These are found to be in good agreement with those obtained from electromagnetic measurements (see Table IV). Therefore a real conclusive test as to the nature of the 0_2^+ band has to await the availability of cross section data for the 2_1^+ state which when included in the full CC scheme calculation should lead to a sensitive determination of β_2^β.

In the case of the 3_1^- state, the performed CC calculations were found to be sensitive to the different K values assumed for the octupole band. This made it possible to assign $K^\pi=3^-$ to the 3_1^- level. The data of the 3_1^- state are then completely reproduced and an octupole deformation parameter $\eta_{33}=0.35$ is deduced; a 30% higher value is required if $K^\pi=0^-$ is assumed instead. The octupole deformation parameter $\eta_{33}=0.35$ leads, using the real part of form factor (7), to a $ME(E3)=26.3\ e\,\mathrm{fm}^3$ in good agreement with the value obtained from electron scattering measurements[28] as well as with the theoretical prediction of the 3-α RGM calculation.[11]

A comparison of the present data with microscopic CC calculations has also been given. The transition potentials were obtained by folding the mass transition densities of the levels of interest with effective nucleon-nucleon interactions. The mass transition densities were obtained from the 3-α RGM wave functions.[11] The comparison has shown that, in these CC calculations imaginary transition potential terms obtained from the phenomenological OM potential were useful in obtaining better fits to the data. Moreover, it is found that for the incident energies of this work, the best nucleon-nucleon interactions that would generate folding transition potentials which would best fit the data are the $M3Y$ interactions (IV) and (VI) and also the simple Yukawa potential[36] (V) without exchange effects.

In conclusion, CC analysis in the rotor-vibrator model for the description of scattering from low-lying states of ^{12}C was very successful both in reproducing the differential cross sections as well as the multipole moments as obtained from electromagnetic measurements. The success of this analysis suggests its application to different mass regions where vibrations are superimposed over statically deformed ground states.

ACKNOWLEDGMENTS

The authors would like to thank M. Kamimura for many useful discussions and for kindly supplying the transition densities and the folding program to deduce the transition potentials. This work was partly performed as part of the research program of the Stichting voor Fundamenteel Onderzoek der Materie (FOM) with financial support from the Nederlandse Organisatie voor Zuiver Wetenschappelijk Onderzoek (ZWO).

[1]K. van der Borg, M. N. Harakeh, and B. S. Nilssøn, Nucl. Phys. A325, 31 (1979); M. N. Harakeh, The code "BEL," Kernfysisch Versneller Instituut report No. 77i, 1981.

[2]L. Ray, G. S. Blanpied, and W. R. Coker, Phys. Rev. C 20, 1236 (1979); G. S. Blanpied, N. M. Hintz, G. S. Kyle, J. W. Palm, R. Liljestrand, M. Bartlett, C. Harvey, G. W. Hoffmann, L. Ray, and D. G. Madland, *ibid.* 20, 1490 (1979); T. Tamura, Rev. Mod. Phys. 37, 679 (1965); Nucl. Phys. 73, 241 (1965).

[3]M. N. Harakeh and R. De Leo, Phys. Lett. 117B, 377 (1982).

[4]L. W. Put and M. N. Harakeh, Phys. Lett. 119B, 253 (1982).

[5]G. S. Blanpied, N. M. Hintz, G. S. Kyle, M. A. Franey, S. J. Seestrom-Morris, R. W. Owen, J. W. Palm, D. Dehnhard, M. L. Barlett, C. Harvey, G. W. Hoffmann, J. A. McGill, R. P. Liljestrand, and L. Ray, Phys. Rev. C 25, 422 (1982).

[6]R. De Leo, G. D'Erasmo, A. Pantaleo, M. N. Harakeh, S. Micheletti, and M. Pignanelli, Phys. Rev. C 23, 1355 (1981).

[7]L. W. Put and M. N. Harakeh, Kernfysisch Versneller Instituut Annual Report, 1981, p. 10 (unpublished).

[8]H. P. Morsch, Phys. Lett. 61B, 15 (1976); B. Castel and G. R. Satchler, *ibid.* 80B, 13 (1978).

[9]H. P. Morsch and P. Decowski, Phys. Lett. 82B, 1 (1979).

[10]K. van der Borg, M. N. Harakeh, and A. van der Woude, Nucl. Phys. A365, 243 (1981); T. Yamagata, K. Iwamoto, S. Kishimoto, B. Saeki, K. Yuasa, M. Tanaka, T. Fukuda, K. Okada, I. Miura, M. Inone, and H. Ogata, Phys. Rev. Lett. 40, 1628 (1978); D. Lebrun, M. Buenerd, P. Martin, P. deSaintignon, and G. Perrin, Phys. Lett. 97B, 358 (1980).

[11]M. Kamimura, Nucl. Phys. A351, 456 (1981).

[12]The code "CHUCK," P. D. Kunz, University of Colorado (unpublished); the program has been modified to incorporate couplings of the β, γ, and octupole bands.

[13]P. D. Greaves, V. Hnizdo, J. Lowe, and O. Karban, Nucl. Phys. A179, 1 (1972).

[14]R. De Leo, G. D'Erasmo, E. M. Fiore, G. Guarino, A. Pantaleo, S. Micheletti, M. Pignanelli, and L. Serafini, Phys. Rev. C 25, 107 (1982).

[15]The code "ECIS," J. Raynal, private communication.

[16]G. A. Grin, C. Joseph, C. Y. Wong, and T. Tamura, Phys. Lett. 25B, 387 (1967).

[17]O. Mikoshiba, T. Terasawa, and M. Tanifuji, Nucl. Phys. A168, 417 (1971).

[18]L. Ray, G. S. Blanpied, W. R. Coker, R. P. Liljestrand, and G. W. Hoffmann, Phys. Rev. Lett. 40, 1547 (1978).

[19]G. S. Blanpied, G. W. Hoffmann, M. L. Barlett, J. A. McGill, S. J. Greene, L. Ray, O. B. Van Dyck, J. Amann, and H. A. Thiessen, Phys. Rev. C 23, 2599 (1981).

[20]The most recent analysis of ^{12}C data at $E_p=800$ MeV, using program ECIS; G. S. Blanpied (private communication).

[21]O. Aspelund, G. Hrehuss, A. Kiss, K. T. Knöpfle, C. Mayer-Böricke, M. Rogge, U. Schwinn, Z. Seres, and P. Turek, Nucl. Phys. A253, 263 (1975).

[22]M. Yasue, T. Tanabe, F. Soga, J. Kokame, F. Shimokoshi, J. Kasagi, Y. Toba, Y. Kadota, T. Ohsawa, and K. Furuno, Nucl. Phys. A394, 29 (1983).
[23]A. Nakada, Y. Torizuka, and Y. Horikawa, Phys. Rev. Lett. 27, 745 (1971); 27, 1102(E) (1971).
[24]Y. Abgrall, B. Morand, and E. Caurier, Nucl. Phys. A192, 372 (1972).
[25]M. Pignanelli, H. V. Geramb, and R. De Leo, Phys. Rev. C 24, 368 (1981), and references therein.
[26]R. De Leo, G. D'Erasmo, F. Ferrero, A. Pantaleo, and M. Pignanelli, Nucl. Phys. A254, 156 (1975).
[27]G. R. Satchler, Part. Nucl. 5, 105 (1972).
[28]H. Crannel, J. T. O'Brien, and D. I. Sober, in *Proceedings of the International Conference on Nuclear Physics with Electromagnetic Interactions, Mainz, 1979,* edited by H. Arenhovel and D. Dreschsel (Springer, Berlin, 1979).
[29]F. Ajzenberg-Selove and C. L. Busch, Nucl. Phys. A336, 1 (1980).
[30]P. Strehl, Z. Phys. 234, 416 (1970).
[31]N. Takigawa and A. Arima, Nucl. Phys. A168, 593 (1971).
[32]J. M. Blatt and J. D. Jackson, Phys. Rev. 76, 18 (1949).
[33]A. B. Volkov, Nucl. Phys. 74, 33 (1965).
[34]A. Hasegawa and S. Nagata, Prog. Theor. Phys. 45, 1786 (1971).
[35]G. R. Satchler and W. G. Love, Phys. Lett. 65B, 415 (1976); G. Bertsch, J. Borysowicz, H. McManus, and W. G. Love, Nucl. Phys. A284, 399 (1977).
[36]T. Nojiri, M. Kamimura, M. Sano, M. Wakai, and K. Yoro, Prog. Theor. Phys. 66, 1906 (1981).
[37]R. S. Mackintosh, Nucl. Phys. A266, 379 (1976); L. W. Owen and G. R. Satchler, *ibid.* 51, 155 (1964).
[38]G. R. Satchler, J. Math. Phys. 13, 1118 (1972).